Supplementary material

Performance Enhancement of Perovskite Solar Cells by Doping Non-Toxic Multifunctional Natural Sodium Lignosulfonate into SnO_2

Zezhuan Jiang [a, 1], Fuling Li [a, 1], Huaiqing Yan [b], Rathes Kannan Ramar [a], Lijia Chen [c], Ping Li [b*] and Qunliang Song [a*]

[a] Institute for Clean Energy and Advanced Materials, School of Materials and Energy, Southwest University, Chongqing Key Laboratory for Advanced Materials and Technologies of Clean Energy, Chongqing 400715, P. R. China.

[b] School of Physics and Electronic Science, Zunyi Normal University, Zunyi 563006, P. R. China.

[c] College of Physics and Electronic Engineering, Chongqing Normal University, Chongqing 401331, P. R. China.

This file includes:

Figure S1 to S16, Table S1 to S6.

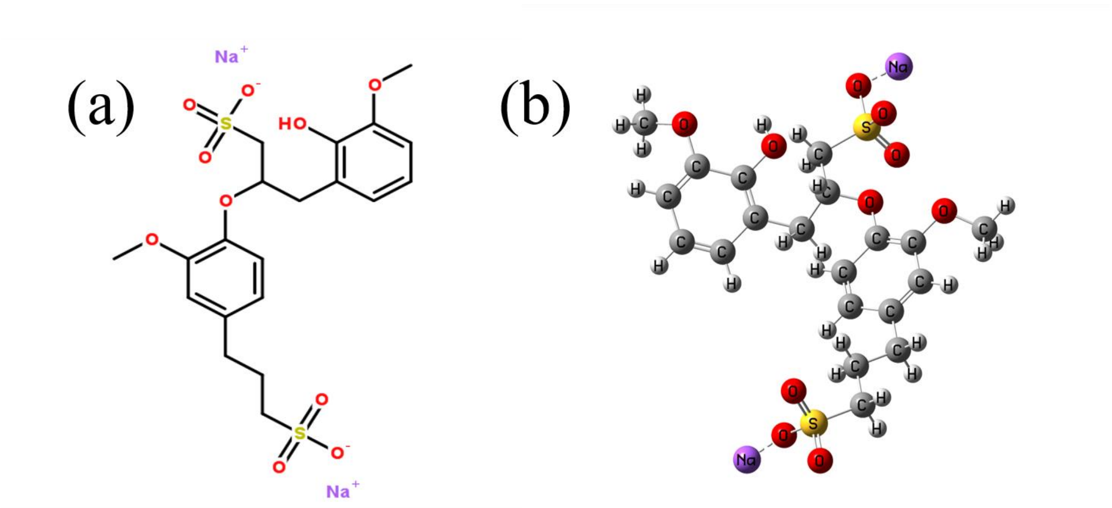

Figure S1. (a) Molecular structure diagram and (b) molecular model diagram of SL.

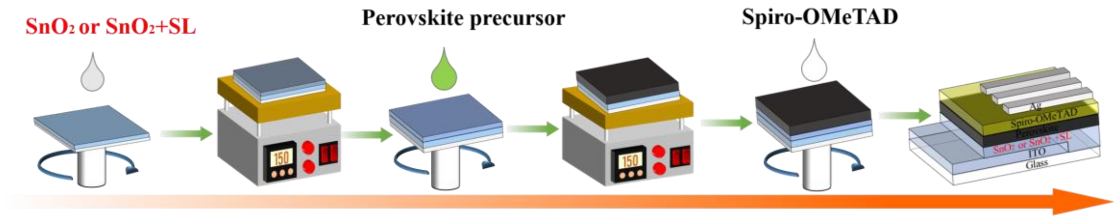

Figure S2. The preparation process of the perovskite solar cells based on SL doped SnO_2 layer.

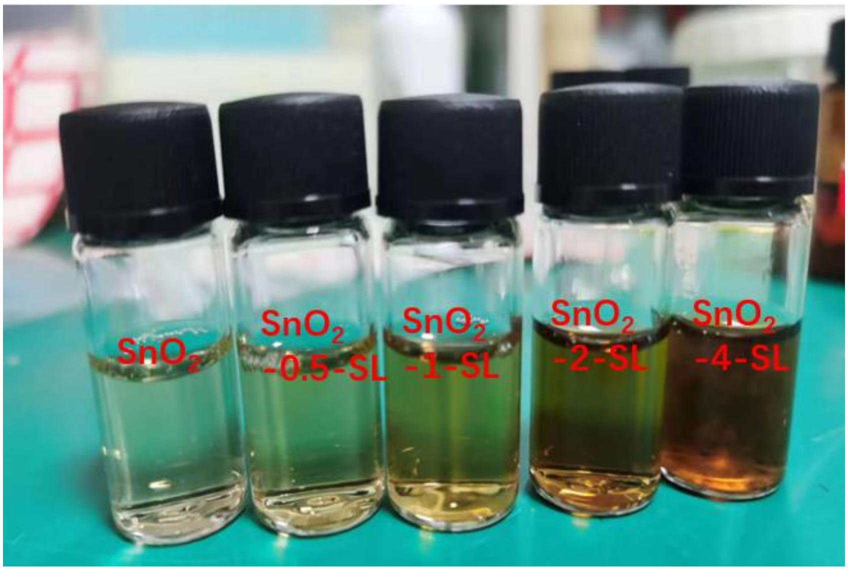

Figure S3. The digital photos of SnO_2 aqueous solutions without and with different concentrations of SL doping.

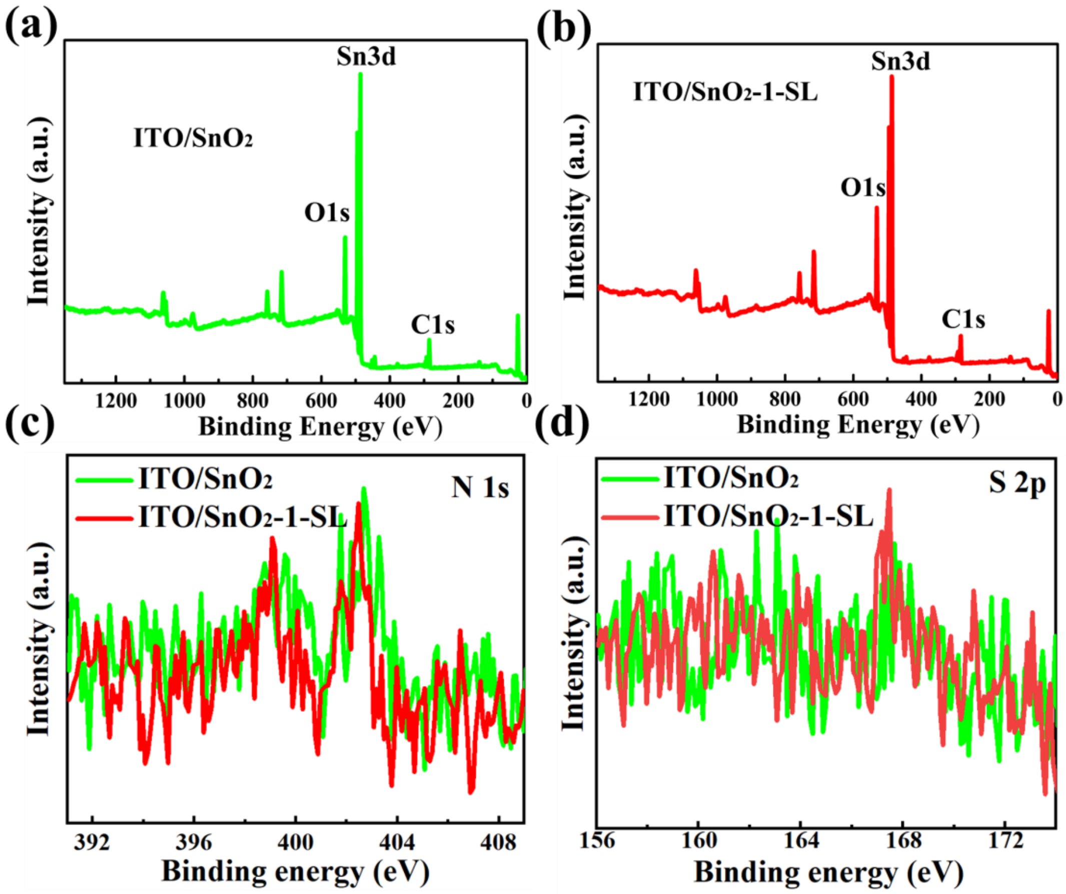

Figure S4. XPS survey spectra of ETL films prepared by (a) SnO_2 and (b) SL-doped SnO_2 solutions, respectively. N 1s spectra (c) and (d) S 2s spectra of pristine and 1-SL doped SnO_2.

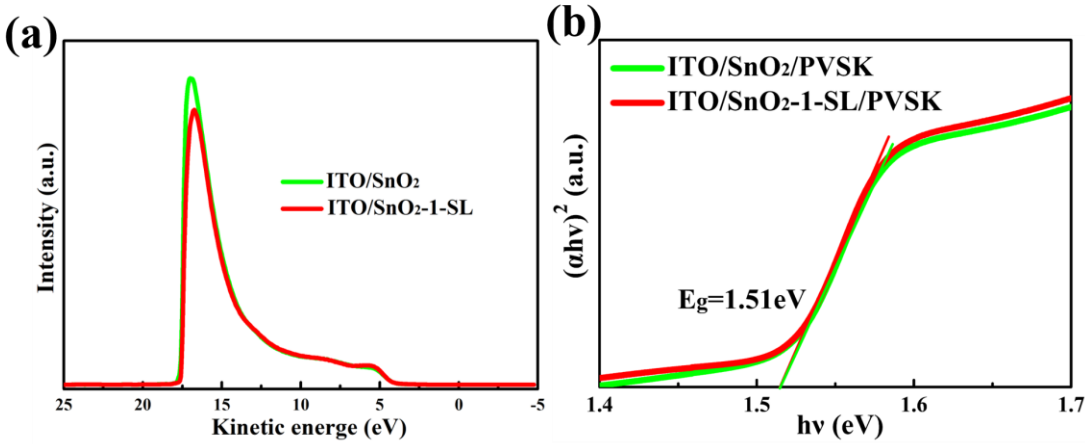

Figure S5. (a) UPS spectra of pristine SnO_2 and 1-SL-doped SnO_2 ETLs, respectively. (b) The optical band gaps of perovskite films of pristine SnO_2 and 1-SL-doped SnO_2 ETLs.

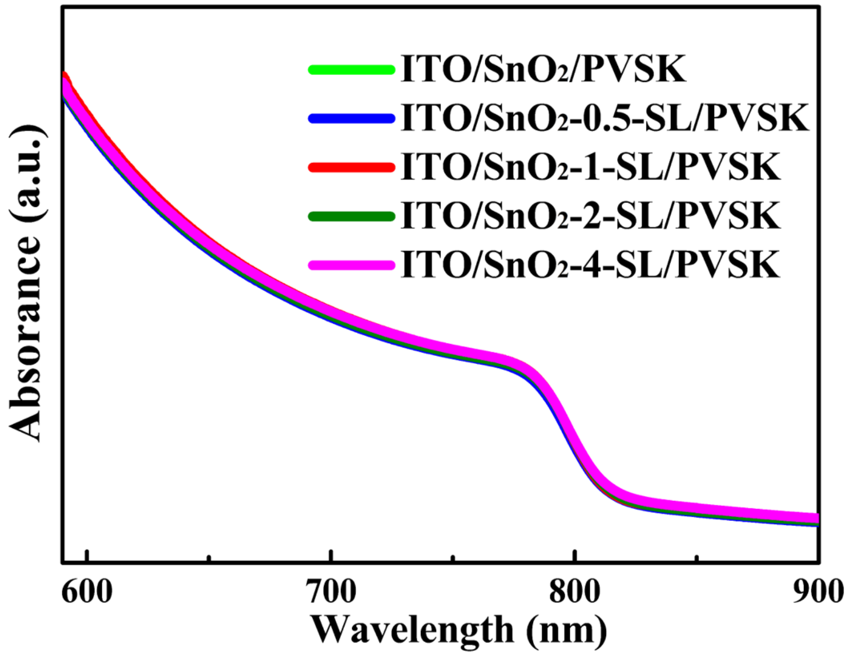

Figure S6. UV-Vis absorption of perovskite films deposited on the pristine SnO_2 and SL-doped SnO_2 ETLs.

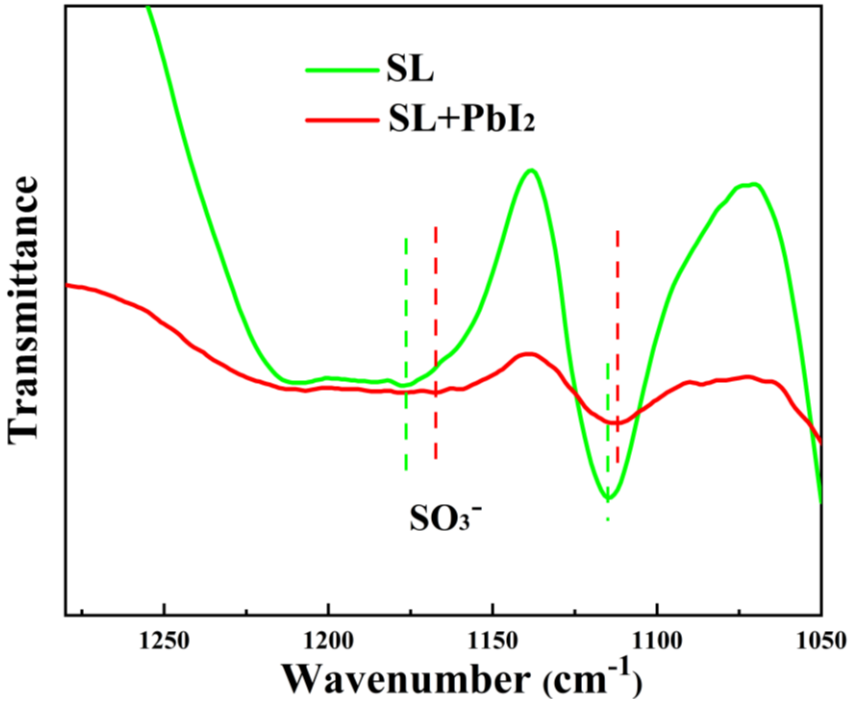

Figure S7. FTIR spectra of SL and SL+PbI_2. The stretching vibration peak of the S=O bond in the SL is located at 1115 cm^{-1}, while in SL+PbI_2 this peak position is shifted to 1111 cm^{-1}.

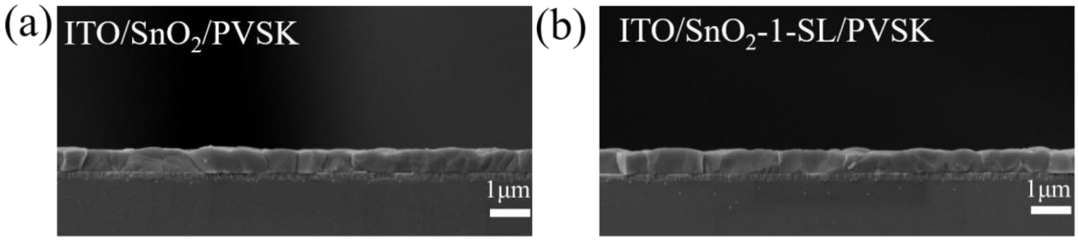

Figure S8. Cross sectional SEM images of the perovskite films based on (a) pristine SnO_2 and (b) 1-SL doped SnO_2.

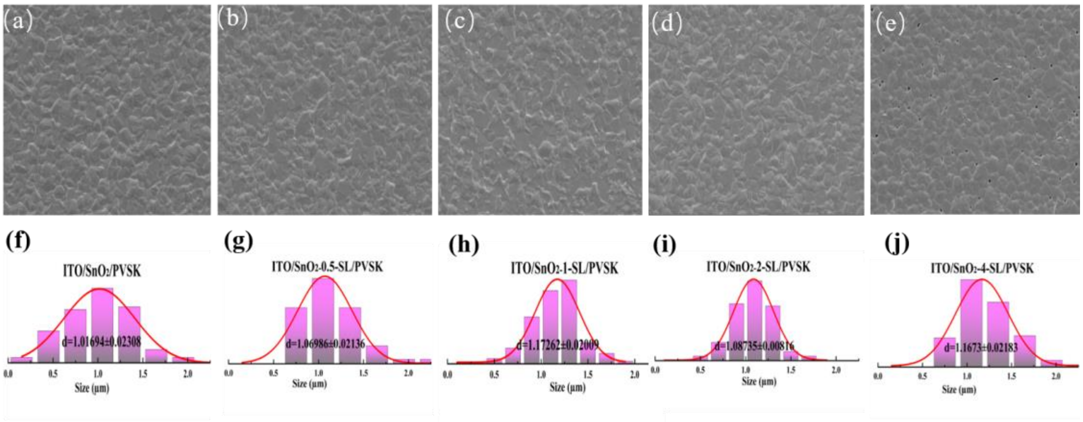

Figure S9. (a) Top-view SEM images of the perovskite films based on (a) pristine SnO_2 and (b) 0.5-SL, (c) 1-SL, (d) 2-SL, (e) 4-SL doped SnO_2. The grains size statistics of perovskite films based on (f) pristine SnO_2 and (g) 0.5-SL, (h) 1-SL, (i) 2-SL, (j) 4-SL doped SnO_2. The scale bar is 1 μm.

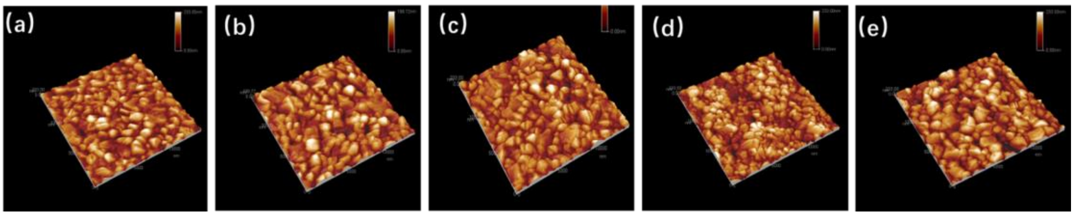

Figure S10. Three-dimensional AFM images of perovskite films based on (a) pristine SnO_2 and (b) 0.5-SL, (c) 1-SL, (d) 2-SL, (e) 4-SL doped SnO_2.

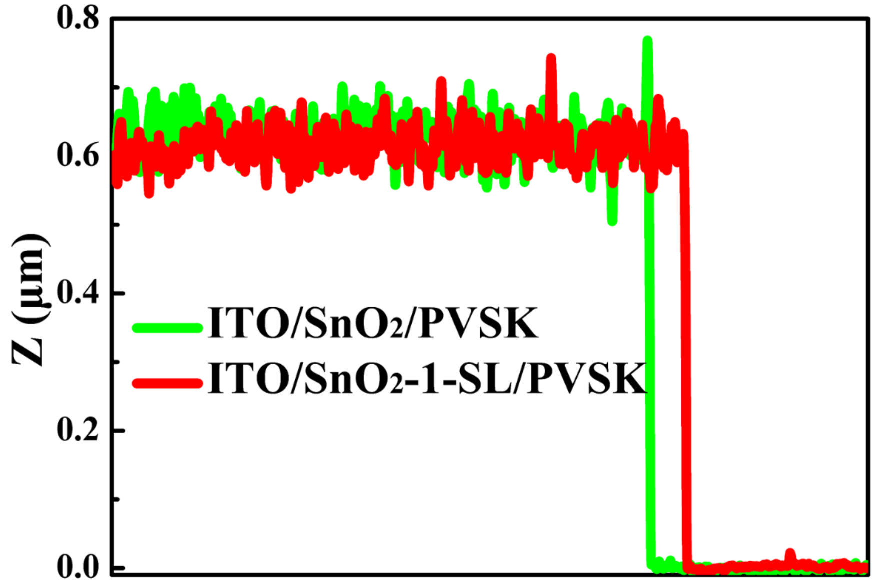

Figure S11. The thicknesses of perovskite layers on pristine and 1-SL treated SnO_2 films.

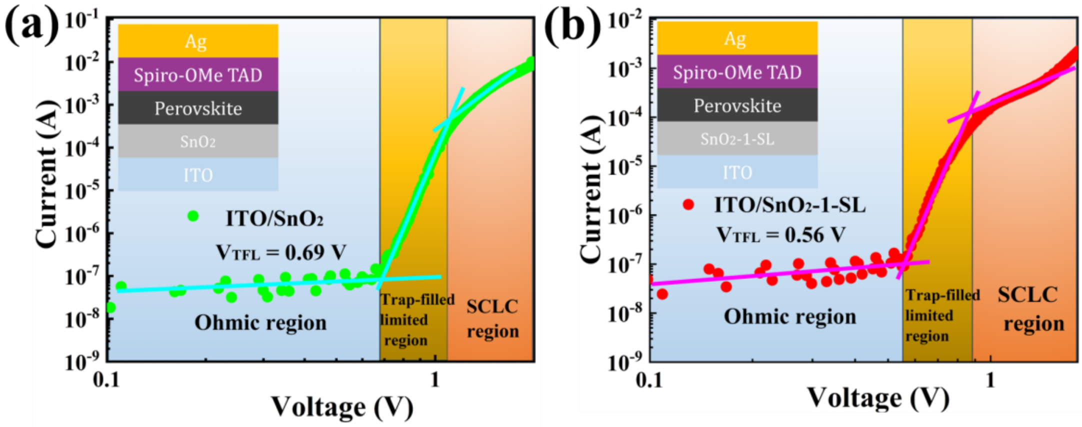

Figure S12. Dark J-V curves of the normal devices with the structures of (a) ITO/SnO_2/perovskite/spiro-OMeTAD/Ag and (b) ITO/SnO_2-1-SL/perovskite/spiro-OMeTAD/Ag.

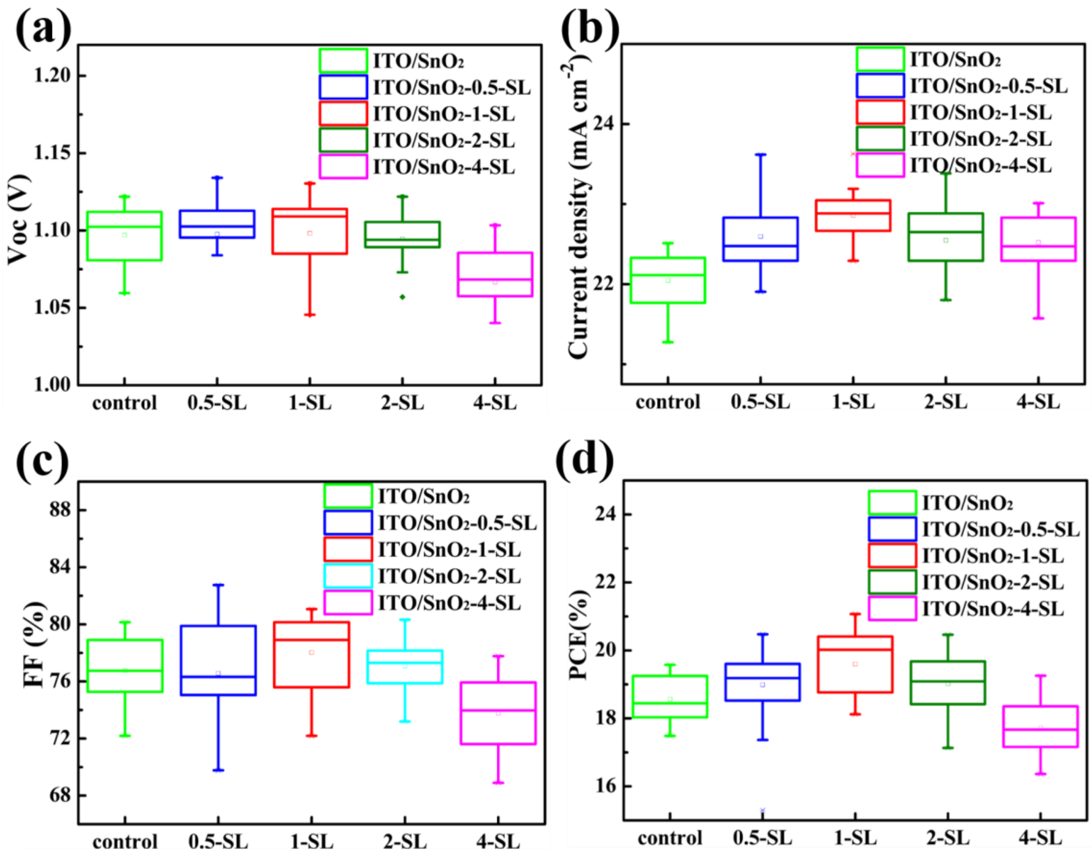

Figure S13. The statistical box charts for the photovoltaic parameters of PSCs based on pristine SnO_2 or SL doped ETLs of (a) V_{oc}, (b) J_{sc}, (c) FF, and (d) PCE.

(a) 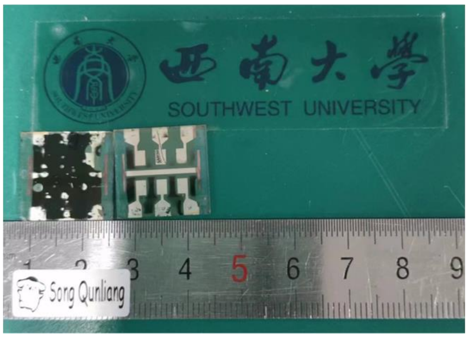 (b) 

Figure S14. The digital photos of perovskite solar cells device after storing in ambient for 840 h at ~20% RH based on (a) pristine SnO_2 and (b) 1-SL-doped SnO_2 ETLs. The SnO_2-1-SL device maintained a relatively intact perovskite morphology.

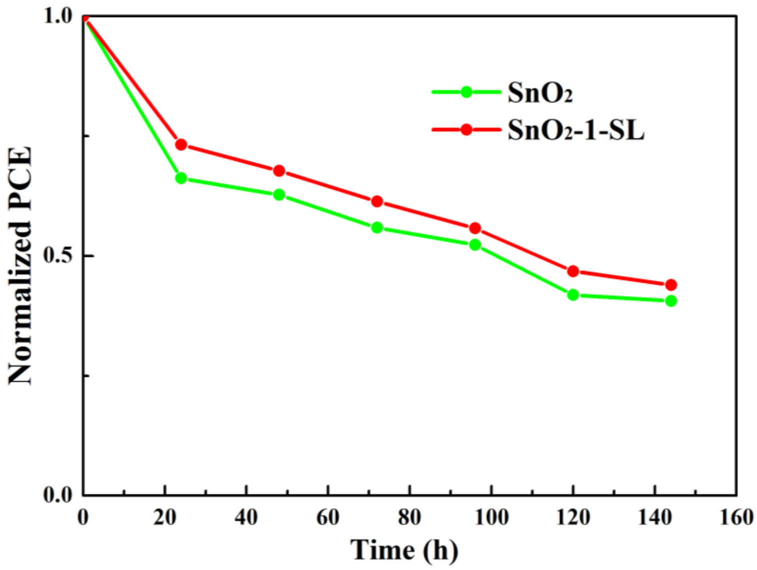

Figure S15. Long-term photostability curves of the PSCs monitored under continuous illumination in glove box.

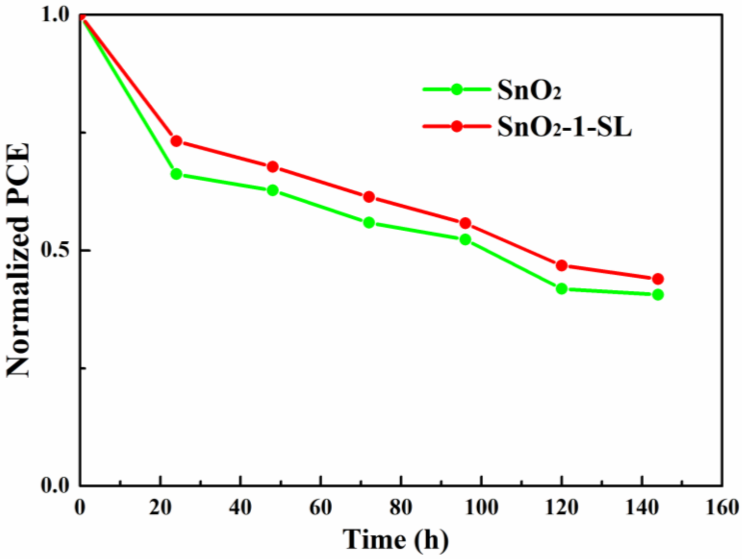

Figure S16. Long-term thermal stability curves of the PSCs monitored at elevated temperature of 65 ℃.

Table S1. The average particle size measured by dynamic light scattering and Zeta potential of pristine SnO_2 and 1-SL-doped SnO_2 precursors.

Samples	Particle size (nm)	Zeta potential (mV)
SnO_2	14.97	-28.83
SnO_2-1-SL	14.95	-30.50

Table S2. FWHM of different XRD diffraction peaks of perovskite films deposited on SnO_2 and SL doped SnO_2 substrates.

Samples	Peak position (degree)	Plane	FWHM (degree)
ITO/SnO_2/PVSK	13.97	(001)	0.129
	28.12	(002)	0.165
ITO/SnO_2-1-SL/PVSK	13.97	(001)	0.125
	28.12	(002)	0.169

Table S3. V_{TFL}, relative dielectric constant (ε_r), thickness, and trap density (N_t) of perovskite films based on pristine SnO_2 or SL treated SnO_2 ETLs.

Samples	V_{TFL} (V)	ε_r	L (nm)	N_t ($\times 10^{15}$ cm^{-3})
SnO_2	0.275	30.8	610	2.60
SnO_2-1-SL	0.185	30.8	610	1.75

Table S4. The fitted EIS parameters of the devices based on pristine SnO_2 and SnO_2-1-SL ETLs, respectively.

Samples	R_s (Ω)	R_{sc} (Ω)	R_{rec} (Ω)
SnO_2	39.73	279.3	1051
SnO_2-1-SL	29.09	265.9	1296

Table S5. Photovoltaic parameters of devices based on SnO_2 ETL doped with different concentrations of SL ranging from 0 to 4 mg·mL^{-1}. Statistics for each concentration were obtained from 20 individual cells. The measurements were conducted under reverse scan.

Devices (mg/mL)		V_{OC} (V)	J_{SC} (mA·cm^{-2})	FF (%)	PCE (%)
Control	Champion	1.111	22.38	78.90	19.60
	Average	1.095 (±0.017)	22.04 (±0.421)	76.76 (±1.16)	19.22 (±0.29)
0.5	Champion	1.110	23.04	79.89	20.47
	Average	1.097 (±0.013)	22.59 (±0.31)	76.92 (±0.90)	19.76 (±0.27)
1.0	Champion	1.112	23.62	80.21	21.12
	Average	1.110 (±0.009)	22.96 (±0.29)	78.92 (±0.73)	20.35 (±0.13)
2.0	Champion	1.110	23.06	80.22	20.58
	Average	1.094 (±0.016)	22.54 (±0.16)	77.46 (±1.03)	19.81 (±0.38)
4.0	Champion	1.090	22.69	77.77	19.25
	Average	1.067(±0.030)	22.52(±0.20)	73.77 (±2.16)	18.63 (±0.39)

Table S6. Summary of the photovoltaic parameters of state-of-the-art devices based on doping SnO_2 solution or SnO_2 treatment.

SnO_2 modification	PSC configuration	J_{sc} (mA cm^{-2})	V_{oc} (V)	FF (%)	PCE (%)	Ref.
NaCl treatment	ITO/SnO_2/NaCl/$MAPbI_3$/Spiro-MeOTAD/Au	22.73	1.06	77.59	18.67	[1]
KOH treatment	FTO/SnO_2/KOH/$Cs_{0.05}(FA_{0.85}MA_{0.15})_{0.95}$ $Pb(I_{0.85}Br_{0.15})_3$/Spiro-MeOTAD/Au	22.60	1.15	79.00	20.50	[2]
Glycine treatment	ITO/SnO_2/Glycine/$Cs_{0.05}MA_yFA_{0.95-y}$ $PbI_{3-x}Cl_x$/Spiro-MeOTAD/Ag	24.15	1.10	78.00	20.68	[3]
Li doping SnO_2	FTO/Li:SnO_2/$MAPbI_3$/Spiro-MeOTAD/Au	23.27	1.11	70.71	18.20	[4]
F doping SnO_2	TO/F:SnO_2/$(FAPbI_3)$0.85(MAPbBr3)0.15/ Spiro-MeOTAD/Au	22.92	1.13	78.05	20.20	[5]
KPAB doping SnO_2	ITO/KPAB:SnO_2/ $Cs_{0.05}FA_{0.85}MA_{0.10}Pb(I_{0.97}Br_{0.03})_3$/ Spiro-MeOTAD/Ag	23.65	1.05	76.6	19.03	[6]
KFBS treatment	ITO/SnO_2/ KFBS/ $FA_{1-x}MA_xPbI_3$ / Spiro-MeOTAD/Ag	24.83	1.14	81.71	23.21	[7]
SLdoping SnO_2	ITO/SL:SnO_2/$FAPbI_3$/Spiro-MeOTAD/Ag	23.62	1.11	80.21	21.12	This work

References

[1] Y. Huang, S. Li, C. Wu, S. Wang, C. Wang, R. Ma, *New J. Chem.*, 2020, 44, 8902-8909.

[2] T. Bu, J. Li, F. Zheng, W. Chen, X. Wen, Z. Ku, Y. Peng, J. Zhong, Y. B. Cheng, F. Huang, *Nat. Commun.*, 2018, 9, 4609.

[3] M. Yu, L. Chen, G. Li, C. Xu, C. Luo, M. Wang, G. Wang, Y. Yao, L. Liao, S. Zhang, Q. Song, *RSC Adv.*, 2020, 10, 19513.

[4] M. Park, J.-Y. Kim, H. J. Son, C.-H. Lee, S. S. Jang, M. J. Ko, *Nano Energym.*, 2016, 26, 208-215.

[5] X. Gong, Q. Sun, S. Liu, P. Liao, Y. Shen, C. Gra, S. M. Zakeeruddin, M. Gra, M. Wang, *Nano Lett*., 2018, 18, 6, 3969–3977.

[6] L. L. Qiu; L. Chen; W. H. Chen; Y. F. Yuan; L. X. Song, D. Q. Mei; B. Bai; F. Q. Xie; P. Du; J. Xiong, ChemElectroChem., 2021, e202101483.

[7] Z. H. Wu, J. H. Wu, S. B. Wang, C. Y. Wang, Y. T. N. Du, Y. Wang, J. L. Geng, Y. H. Lin, W. H. Sun, Z. Lan, *Chem. Eng. J*., 2022, 449, 137851.